Anharmonicity in a Double Hydrogen Transfer Reaction Studied in a Single Porphycene Molecule on a Cu(110) Surface

S. Liu,[1, ¶] D. Baugh,[1, ¶, †] K. Motobayashi,[2] X. Zhao,[3] S. V. Levchenko,[3, 4] S. Gawinkowski,[5] J. Waluk,[5, 6] L. Grill,[7] M. Persson,[8] and T. Kumagai[1,*]

[1] Department of Physical Chemistry, Fritz-Haber Institute of the Max-Planck Society, Faradayweg 4-6, 14195 Berlin, Germany

[2] Department of Physical Science and Engineering, Nagoya Institute of Technology, Gokiso, Showa, Nagoya 466-8555, Japan

[3] Theory Department, Fritz-Haber Institute of the Max-Planck Society, Faradayweg 4-6, 14195 Berlin, Germany

[4] Laboratory of Modelling and Development of New Materials, NUST MISIS, Leninskiy prospekt 4, Moscow 119049, Russia

[5] Institute of Physical Chemistry, Polish Academy of Sciences, Kasprzaka 44/52, Warsaw 01-224, Poland

[6] Faculty of Mathematics and Natural Sciences, College of Science, Cardinal Stefan Wyszyński University, Dewajtis 5, 01-815 Warsaw, Poland

[7] Department of Physical Chemistry, University of Graz, Heinrichstrasse 28, 8010 Graz, Austria

[8] Surface Science Research Centre and Department of Chemistry, University of Liverpool, Liverpool L69 3BX, UK

Anharmonicity plays a crucial role in hydrogen transfer reactions in hydrogen-bonding systems, which leads to a peculiar spectral line shape of the hydrogen stretching mode as well as highly complex intra/intermolecular vibrational energy relaxation. Single-molecule study with a well-defined model is necessary to elucidate a fundamental mechanism. Recent low-temperature scanning tunnelling microscopy (STM) experiment revealed that the *cis* ↔ *cis* tautomerization in a single porphycene molecule on Cu(110) at 5 K can be induced by vibrational excitation via an inelastic electron tunnelling process and the N–H(D) stretching mode couples with the tautomerization coordinate [Kumagai *et al. Phys. Rev. Lett.* 2013, 111, 246101]. Here we discuss a pronounced anharmonicity of the N–H stretching mode observed in the STM action spectra and the conductance spectra. The density functional theory calculations find a strong intermode coupling of the N–H stretching with an in-plane bending mode within porphycene on Cu(110).

KEYWORDS: Tautomerization, Single-molecule vibrational spectroscopy, Anharmonicity, Surface Science, Scanning tunnelling microscopy, Porphycene

Hydrogen (H) transfer reactions are of fundamental importance in nature.[1] The H transfer dynamics is complicated by anharmonic potential energy surfaces caused by the hydrogen bond which act as a pathway of H atoms. The anharmonicity results in a strong intermode coupling of the A–H stretching (A is an electronegative atom) with the other lower frequency modes, which leads to highly complex spectral features in vibrational spectra, particularly in the stretching band.[2] Although anharmonicity in H-bonding systems has been studied extensively by vibrational spectroscopy and quantum chemical calculations,[3] an accurate and quantitative description of the peculiar vibrational spectral features as well as the H-transfer dynamics remains a challenging topic. Since the anharmonic nature is hidden by inhomogeneous effects in bulk samples, it is essential to study a well-defined model and/or employ local spectroscopy down to the single-molecule level. Intramolecular hydrogen transfer reactions, so-called tautomerization, have served as an important model for studying a fundamental mechanism of H-transfer dynamics.[4] Porphycene has been examined as a model of a double H-transfer that occurs in a shallow and strongly anharmonic potential energy surface resulting from the strong intramolecular hydrogen bonds.[5, 6, 7, 8] Recent low-temperature scanning tunnelling microscopy (STM) experiment revealed that the *cis* ↔ *cis* tautomerization of a single porphycene molecule on Cu(110) can be induced by vibrational excitation via inelastic

electron tunnelling and that the N–H stretching mode couples with the tautomerization coordinate.[9] The DFT calculations were used to determine the adsorption structure and also proposed that the *cis–cis* tautomerization occurs by a stepwise mechanism in which the meta-stable *trans* configuration is involved as an intermediate state along the reaction pathway.[9, 10, 11] Here we provide an in-depth analysis of single-molecule vibrational spectroscopy with STM and discuss a pronounced anharmonicity of the N–H stretching mode.

RESULTS AND DISCUSSION

Figure 1a shows STM images of the initial and final states of the *cis* ↔ *cis* tautomerization of a single porphyence on Cu(110) at 5 K.[9, 10] The electron-induced tautomerization of porphycene is studied by STM action spectroscopy (STM-AS) which has emerged as a powerful method to study single-molecule reactions on surfaces.[12, 13] We measured STM-AS for normal (*h*-porphycene) and deuterated porphycene (d_2-porphycene in which only the inner H atoms are replaced by D)[9] and the spectral fitting analysis is carried out using an established method.[12, 13] This fitting analysis enables us to extract the vibrational properties of molecular adsorbates which is associated with the reaction. The reaction yield Y at a specific bias voltage V is defined by

$$Y = \frac{R}{I_t/e}, \quad (1)$$

where R is the reaction rate, I_t the tunnelling current, and e the elementary charge. At constant V, R follows a power law dependence,[14]

$$R \propto I_t^N, \quad (2)$$

where N is the total reaction order, *i.e.*, the number of the tunnelling electron required to trigger the reaction. Theoretically the reaction rate is given by the vibrational generation rate (Γ_{iet}) via an inelastic electron tunnelling process.[15] Γ_{iet} can be expressed as a convolution of the vibrational density of states (DOS, $\rho_{ph}(\omega)$) and the spectral generation rate function (Γ_{in}): $\Gamma_{iet}(V) = \int_0^\infty d\omega \rho_{ph}(\omega)\, \Gamma_{in}(\omega)$, as derived in Ref. 15. $Y(V)$ can be expressed using double integration of vibrational DOS as

$$Y(V) = K\frac{f(V)^n}{V}, \quad (3)$$

$$f(V) = \frac{1}{e}\int_0^{eV} d\omega \int_0^{\omega} \rho_{ph}(\omega')d\omega', \quad (4)$$

where K is the prefactor (rate constant) that is determined by the elementary process behind the reaction and n is the reaction order of vibrational excitation. If several vibrational modes are involved in STM-AS, the total reaction yield $Y_{tot}(V)$ becomes the summation $Y(V)$ from each active vibrational mode i with energy $\hbar\Omega_i$,[12, 13, 16]

$$Y_{tot}(V) = \sum_i K_i \frac{f_i(V)^{n_i}}{V}. \quad (5)$$

When the reaction is induced by simultaneous excitation of several different vibrational

modes, the total reaction order (N) involves contribution from each excitation. Fitting analysis of $Y(V)$ using Eq. (5) has been employed to extract the energy and broadening factor of active vibration modes.[17, 18, 19, 20, 21] Here we use a Gaussian function $\rho_{\mathrm{ph}}(\omega) = \frac{1}{\sqrt{2\pi}\sigma_i}\exp\left(-\frac{(\omega-\Omega_i)^2}{2\sigma_i^2}\right)$ because it allows to taking into account broadening effects including all possible contributions, *i.e.*, finite temperatures, vibrational relaxation, instrumental resolution,[12] and anharmonic effects due to hydrogen bonding.[16] The full width of half maximum (γ_i) of the Gaussian vibrational DOS is given by $\gamma_i = 2\sqrt{2\ln 2}\sigma_i$.

We first discuss the STM-AS for the *cis* ↔ *cis* tautomerization of d_2-porphycene (**Fig. 1b**). The lateral tip position during the measurement is indicated in **Fig. 1a**, which corresponds to the side of pyrrole rings with the amine N atoms. **Figure 1c** shows the current dependence of the tautomerization rate, where N changes from ~2 to ~1 around 260 mV. Thus, tautomerization occurs via a two- and a one-electron process at the low and high voltage regimes, respectively. At higher currents, the tip–molecule distance becomes smaller and the STM tip may affect the tautomerization through the interaction with the molecule, which eventually leads to modification of the potential energy surface.[11] However, the modification is expected to be rather small at the tip–molecule distances in this experiment (the tip is substantially far from the equilibrium distance in the tip–molecule potential, where the significant deformation of the potential occurs[11]).

Hence, the influence on the reaction order should be negligible. Since the tautomerization rate is very small at low bias voltages, we used a relatively high current to measure the yields (see the lower panel of **Fig. 1b**) in order to observe a sufficient number of tautomerization events in a realistic time-scale of the experiment. However, according to Eq. (1) and (2), $Y(V)$ depends on the current in a multi-electron process, in contrast to a one-electron process. Therefore, the current affects the $Y(V)$ curve at low voltages. The small markers in the upper panel of **Fig. 1b** show the measured (raw) yields (Y_{raw}) obtained at the used tunnelling current (I_{raw}) indicated in the lower panel. In order to examine the influence of the current to the $Y(V)$ curve, we test the following normalization. The open markers in **Fig. 1b** are the yields (Y_{norm}) normalized to a specific current (I_{norm}: 0.1, 1, and 10 nA), which is given by $Y_{\mathrm{norm}} = \frac{I_{\mathrm{norm}}^{N-1}}{I_{\mathrm{raw}}^{N-1}} Y_{\mathrm{raw}}$ where N was obtained from a fitting analysis of the current dependence measurement (*cf.* **Fig. 2b**). These values for I_{norm} are in a typical range of tunnelling currents in STM. We do not take into account any influence of the tip–molecule interaction that may modify the potential energy surface of the tautomerization.[11] Note that this normalization was not carried out in our previous report.[9] As discussed later (*cf.* **Fig. 2c**), N may be varied depending on the measured current range when one- and two-electron processes are simultaneously involved. The consistency of the normalized yield was confirmed at several bias voltages where the

current dependence of the rate is available (**Fig. 1c**). It is clear that $Y(V)$ at different currents exhibits a vertical shift in the two-electron regime (**Fig. 1b**), which leads to a critical change in K_i in Eq. (5) but the other vibrational factors, namely the vibrational energy and width, are not significantly influenced in the fitting analysis.

For d_2-porphycene, $Y(V)$ exhibits a threshold at ~160 mV and a second steep increase at ~260 mV. A similar result was obtained at both bias polarities. The solid line in **Fig. 1b** is the best fitting result to Eq. (5) with the parameters listed in **Table 1**. The obtained vibrational energy for the second increase of $Y(V)$ is in excellent agreement with the calculated symmetric (anti-symmetric) N–D stretching mode, $\nu_{s(as)}$(N–D), of 281.9 (280.9) meV. However, the vibrational DOS around the threshold voltage show a large broadening factor which ranges typically from 5 to 15 meV.[13] This broad vibrational DOS may be explained by contribution from several different vibrational excitations. Additionally, the reaction is second order (*i.e.*, two-electron process) at this voltage range, thus multiple excitations of vibrational modes are also involved and the reaction should comprise complex elementary processes.[18] Moreover, a bunch of vibrational modes exist for porphycene below 200 meV,[9] hampering clear assignment of the involved modes. A similar threshold voltage (~150 mV) is also observed for tautomerization of porphycene on Cu(111).[22, 23] A recent theoretical study by Novko *et al.* proposed that the excitation

of skeletal modes plays a crucial role in the process.[24] It should also be noted that the reaction (minimum energy) path for tautomerization on Cu(110) and Cu(111) does not initially involve N-H stretching but rather a small lateral translation of porphycene along the surface.[10, 11, 25] Therefore, the reaction coordinate should also involve low frequency modes such as the hindered translation and rotation of the molecule.

The tautomerization is observed to be enhanced by the ν(N–D) excitation, which suggests that this reaction does not follow the reaction path since this vibrational energy does not appear in low frequency modes along the initial reaction path. The ν(N–D) energy can also be dissipated through electron–hole pair excitation in the substrate as well as intramolecular vibrational relaxation.[26, 27, 28] K_i in Eq. (5), in principle, contains important physical parameters such as vibrational dumping rates of the excited vibrational mode through relaxation to the reaction coordinate, the other low frequency modes (including surface phonons), and electron-hole pair excitation.[29, 30] However, we were unable to extract such valuable information due to the lack of the detailed knowledge of the complex elementary process of tautomerization of porphycene on the surface.

$Y(V)$ of *h*-porphycene shows a conspicuous difference from d_2-porphycene (**Fig. 2a**). Although the threshold at ~150 meV is similar, the second increase of $Y(V)$, which should correspond to the ν(N–H) excitation, is not as obvious as ν(N–H) excitation of d_2-

porphycene. Instead, $Y(V)$ exhibits a very moderate increase ranging from 200 to 380 mV. A similar moderate increase of $Y(V)$ was also observed for the H-bonded O–H stretching mode in a water–hydroxyl complex on Cu(110), which is interpreted as vibrational broadening caused by anharmonic potential.[16] As shown in **Fig. 1b**, $Y(V)$ of d_2-porphycene can be reproduced with Eq. (5) with two vibrational DOS, that is, excitation of skeletal modes at 181.3 meV and ν(N–D) at 274.7 meV. Using the simple harmonic approximation, the ν(N–H) energy can be estimated to be 375 meV from the ν(N–D) energy,[31] which is in excellent agreement with the simulated ν(N–H) at 376 mV by DFT.[9] However, if the STM-AS of *h*-porphycene is simulated with Eq. (5) using two vibrational DOS for skeletal mode excitations around the threshold voltage and ν(N–H) around 375 meV with a comparable broadening factor obtained for d_2-porphycene, the resulting curve largely deviates from the experimental result (see the red dashed line in **Fig. 2a**).

A remarkable difference between *h*- and d_2-porphycene is also observed in the voltage dependence of N (**Fig. 2b**). The transition from a two- to a one-electron process is relatively sharp for d_2-porphycene, whereas it is much more gradual for *h*-porphycene[32] and the transition spreads from 220 to 270 mV. This gradual transition suggests that the vibrational DOS of a skeletal mode and the N–H stretching are simultaneously excited in this voltage range, resulting in the non-integer N. In this situation, the total reaction rate

is given by[19]

$$R = R_1 + R_2 = k_1 I_t + k_2 I_t^2, \quad (6)$$

where k_1 [$s^{-1}A^{-1}$] and k_2 [$s^{-1}A^{-2}$] are the rate constant for the one- and two-electron process, respectively. In **Fig. 2c**, the current dependence of the tautomerization rate obtained at V_{sample} = –250 mV is fitted by Eq. (6), giving k_1 = 4.99(±0.73) × 10^6 $s^{-1}A^{-1}$ and k_2 = 3.02(±0.30) × 10^{17} $s^{-1}A^{-2}$. At low currents the one-electron process dominates the total rate, whereas the two-electron process prevails at high currents. Therefore, *N* in Eq. (2) is affected by the measured current range when different processes compete. We also note that the second term in Eq. (6) should be more complex because the two-electron process involves various elementary processes.[19, 33] As discussed above, the vibrational DOS around the threshold voltage involve the contribution from multiple vibrational excitations. Thus, an in-depth analysis of k_2 requires precise information about contributions from the individual modes, which is not available in the present case. A detailed theoretical analysis for a complex process including one- and two-electron processes has been applied only to a simple reaction such as rotation of an acetylene molecule on Cu(100).[34]

A remarkable difference between *h*- and d_2-porphycene was also observed in the d*I*/d*V* spectrum,[9] where vibrational signals appear as a characteristic peak or dip (**Fig. 3a**).

The peak and dip at 177 and 284 mV observed for d_2-porphycene nicely match skeletal modes and the ν(N–D) excitation, respectively. These values are also consistent with the fitting parameters of $Y(V)$ (**Table 1**). However, the dI/dV spectrum of *h*-porphycene exhibits rather complex features between 300 and 400 mV consisting of a broad peak and dip, which correspond to the ν(N–H) band. Furthermore, it is found that the dip includes two components in the high-resolution dI/dV spectrum (see inset of **Fig. 3a**). These spectral features suggest the existence of multiple vibrational excitations around ν(N–H). We find that $Y(V)$ of *h*-porphycene can be reproduced using Eq. (5) using at least two vibrational DOS in the ν(N–H) regime where the peak and dip are observed in the dI/dV spectrum. The fitted result is indicated by the solid line in **Fig. 2a** and the fitting parameters are listed in **Table 1**.

The ν(N–H) energy found in the $Y(V)$ and dI/dV spectra appears to be considerably red-shifted as compared to the N–H stretching mode, for example, in NH_3 (417 meV[35]), free-base porphyrin in rare-gas matrices (412 meV[36]), and phthalocyanine on Ag(111) (406 meV[37]), indicating the presence of relatively strong H bonds in porphycene on Cu(110). A vibrational broadening and emergence of additional satellite bands for the A–H stretching mode in H bonding systems are known from IR spectroscopy.[38, 39, 40] The broadening results from anharmonic coupling of this stretching mode with other lower

frequency modes,[39, 41, 42, 43] which leads to modulation of the A–H stretching potential and intramolecular vibrational relaxation because third- and higher-order terms of this potential are enhanced by H bonding. Furthermore, the coupling between the A–H stretching and overtone/combination modes is enhanced by anharmonic resonance, *e.g.*, Fermi resonance.[38, 42, 43, 44]

Since no fundamental mode exists between 200 and 376 meV for *h*-porphycene on Cu(110),[9] the peak at 330 mV in the d*I*/d*V* spectrum observed for *h*-porphycene should be assigned to overtone/combination excitation of lower vibrational modes. The absence of a peak (observed for *h*-porphycene) around the ν(N–D) energy region of d_2-porphycene implies that the peak at 330 mV for *h*-porphycene appears in a similar mechanism to other H-bonding systems (as discussed above) and the coupling may be enhanced through a Fermi resonance between ν(N–H) and the overtone/combination mode(s), most likely N–H bending. Additionally, it is found that the second dip at 385 meV observed in the high-resolution spectrum for *h*-porphycene is absent in d_{12}-porphycene in which all the peripheral H atoms are replaced by D atoms but without any substitution of the inner H atoms (see chemical structure in **Fig. 3b**). This indicates that the first and second dip cannot be assigned to symmetric and anti-symmetric combinations of the fundamental ν(N–H). The possibility of a contribution from C–H stretching modes is also excluded

because the dip is also absent in d_2-porphycene. Therefore, it should also be assigned to the different overtone/combination mode from the one around 330 mV.

The spectral anomalies of ν(N–H) of porphycene on Cu(110) indicate a pronounced effect of the anharmonicity caused by a strong coupling with a lower vibrational mode(s) that can modulate the H-bonding geometry within the molecular cavity. Such a coupling mechanism and vibrational line broadening of ν(N–H) were examined with quantum mechanical calculations for porphycene in the gas phase.[5] Here we have investigated one anharmonic coupling term on the surface by calculating the variation of the ν(N–H) and ν(N–D) energies as a function of the displacement along a lower frequency mode (**Figure 4c**). This mode causes the largest displacement of the N–H···N geometry and is essentially an N–H bending mode (**Fig. 4b**). A considerable variation occurs in the ν(N–H) energy (**Fig. 4c**), indicating strong anharmonic coupling of ν(N–H) with the bending mode. However, this variation is almost negligible for ν(N–D) because the anharmonicity of the potential has lesser impact on ν(N–D) than ν(N–H) due to the larger amplitude of the zero-point motion of the bending mode of N–H than of N–D. Finally, note that our study only indicates that there is a strong anharmonic coupling term for *h*-porphycene compared to d_2-porhpycene but is not intended to describe the anharmonic vibrational line shape and the Fermi resonance. This description would require the calculation of

more anharmonic terms in the coupling between the stretch mode and the bending mode, such as, for instance, the change of the frequency of the low-energy mode with the amplitude of the stretch mode.

CONCLUSIONS

We have presented a detailed analysis of STM-AS for the *cis* ↔ *cis* tautomerization of porphycene isotopologues on a Cu(110) surface at 5 K and have discussed the pronounced anharmonicity of the N–H stretching mode. The spectral fitting analysis of STM-AS in combination with the reaction order measurement revealed the vibrational energies and broadening factors of the involved modes. The tautomerization is induced through multiple excitations of skeletal vibrational modes of porphycene and the N–H(D) stretching largely enhances the reaction. These vibrational excitations were also identified in the conductance spectroscopy, manifested as a peak or dip around the vibrational energy. We found that the N–H stretching mode shows not only a significant broadening, but also an emergence of additional vibrational spectral features which indicate a pronounced anharmonicity and strong coupling with lower frequency modes. In contrast, these spectral anomalies were absent in the N–D stretching mode. Theoretical simulations demonstrated a strong intermode coupling of the N–H stretching with the bending mode

but not for the N–D stretching mode. These results indicate a significantly different contribution of the anharmonicity between the N–H and N–D stretching modes. Our approach paves the way for studying anharmonicity in H-transfer reactions on solid surfaces *at the single-molecule level*.

EXPERIMENTS

All experiments were performed in an ultra-high vacuum chamber (base pressure of 10^{-10} mbar) equipped with a low-temperature STM (modified Omicron instrument with Nanonis Electronics). STM measurements were conducted at 5 K in the constant-current mode with the bias voltage (V_{bias}) applied to the tip (V_{tip}) or sample (V_{sample}). The Cu(110) surface was cleaned by repeated cycles of argon ion sputtering followed by annealing to 700 K. STM tips were made from a tungsten or gold wire and then optimized *in situ* by applying a voltage pulse and controlled indentation of the tip into the surface. Porphycene molecules were deposited onto the surface at room temperature from a Knudsen cell (at a temperature between 450 and 500 K) and the sample was then transferred to the STM at 5 K.

COMPUTATIONAL METHODS

DFT calculations were performed using the Fritz-Haber Institute *ab initio* molecules simulations package (FHI-aims)[45] with the Perdew-Burke-Ernzerhof (PBE) functional[46] and a Monkhorst-Pack[47] *k*-grid of 3×3×1 *k*-points in the supercell. Long-range van der Waals forces were accounted for by the Tkatchenko-Scheffler scheme[48]. An all-electron and a default tight basis set was used. The Cu(110) surface was represented by a four layer slab with a 4 × 6 surface unit cell and a >20 Å vacuum region. The two topmost layers were relaxed and the residual Cu atoms were fixed at the bulk geometry (the lattice constant of 2.568 Å). The vibrations of the adsorbed molecule were calculated on a rigid substrate lattice (the Cu atoms were fixed) by diagonalising the dynamical matrix which was obtained by finite differences of the calculated forces at symmetric ionic displacements of 0.02 Å.

AUTHOR INFORMATION

¶ These authors contributed equally to this work.

† Permanent address: Department of Chemistry & Biochemistry, University of California, Los Angeles, CA 90095-1569. USA

* Corresponding author: kuma@fhi-berlin.mpg.de

Notes

The authors declare no competing financial interest.

ACKNOWLEDGMENTS

The authors thank Mariana Rossi, Martin Wolf, Maki Kawai, and Hiromu Ueba for stimulating discussions. T.K. acknowledges the support of Morino Foundation for Molecular Science. S.V.L is grateful for the support by the Ministry of Education and Science of the Russian Federation in the framework of Increase Competitiveness Program of NUST ‘MISIS’ (No K2-2016-013) implemented by a governmental decree dated 16 March 2013, No 211. S.G. and J.W. acknowledge the support by the Polish National Science Center Grants DEC-2011/02/A/ST5/00043 and DEC-2013/10/M/ST4/00069. D.B. acknowledges the Travel Grant from the UCLA Chancellor’s Office.

Table 1. Fitting parameters of $Y(V)$ for h- and d_2-porphycene.

	K (mV^{1-n})	$\hbar\Omega$ (meV)	γ (meV)	n
d_2-Porphycene				
Skeletal modes	**$(1.53\pm0.24)\times10^{-13}$**	**181.3±3.3**	**54.5±4.9**	**2**
ν(N–D)	**$(2.66\pm0.21)\times10^{-7}$**	**274.7±0.8**	**16.0±2.0**	**1**
h-Porphycene				
Skeletal modes	**$(2.36\pm0.28)\times10^{-12}$**	**168.9±5.6**	**41.4±5.4**	**2**
Overtone or combination	**$(3.20\pm0.53)\times10^{-7}$**	**327***	**76.6±2.8**	**1**
ν(N–H)	**$(5.04\pm0.49)\times10^{-5}$**	**358***	**35.7±1.2**	**1**

*** These values are restricted around the peak and dip position observed in the dI/dV spectrum of h-porphycene in Fig. 3a.**

REFERENCES

[1] J. T. Hynes, J. P. Klinman, H.-H. Limbach, R. L. Schowen (Eds.), Hydrogen-Transfer Reactions, Wiley-VHC, Weinheim, 2007.

[2] D. Hadži (Ed.), Hydrogen Bonding. (Pergamon Press, London, 1959)

[3] G. C. Pimentel, A. L. McLellan, The Hydrogen Bond. (Freeman, San Francisco, 1960).

[4] L. Antonov, Tautomerism: Methods and Theories. Wiley, 2013.

[5] S. Gawinkowski, Ł. Walewski, A. Vdovin, A. Slenczka, S. Rols, M. R. Johnson, B. Lesyng, J. Waluk, Vibrations and hydrogen bonding in porphycene. *Phys. Chem. Chem. Phys.* **2012**, *14*, 5489–5503.

[6] J. Waluk, Ground- and Excited-State Tautomerism in Porphycenes. *Acc. Chem. Res.* **2006**, *39*, 945–952.

[7] J. Waluk, Spectroscopy and tautomerization studies of porphycene, *Chem. Rev.* **2017**, *117*, 2447–2480

[8] P. Fita, L. Grill, A. Listkowski, H. Piwoński, S. Gawinkowski, M. Pszona, J. Sepioł, E. Mengesha, T. Kumagai and J. Waluk, pectroscopic and microscopic investigations of tautomerization in porphycenes: condensed phases, supersonic jets, and single molecule studies. *Phys. Chem. Chem. Phys.* **2017**, *19*, 4921–4937.

[9] T. Kumagai, F. Hanke, S. Gawinkowski, J. Sharp, K. Kotsis, J. Waluk, M. Persson, and L. Grill, Thermally and vibrationally induced tautomerization of single porphycene molecules on a Cu(110) surface. *Phys. Rev. Lett.* **2013**, *111*, 246101.

[10] T. Kumagai, F. Hanke, S. Gawinkowski, J. Sharp, K. Kotsis, J. Waluk, M. Persson, & L. Grill, Controlling intramolecular hydrogen transfer in a porphycene molecule with single atoms or molecules located nearby. *Nat. Chem.* **2014**, *6*, 41–46.

[11] J. N. Ladenthin, T. Frederiksen, M. Persson, J. C. Sharp, S. Gawinkowski, J. Waluk, & T. Kumagai, Force-induced tautomerization in a single molecule. *Nature Chemistry* **2016**, *8*, 935–940.

[12] K. Motobayashi, Y. Kim, H. Ueba, M. Kawai, Insight into Action Spectroscopy for Single Molecule Motion and Reactions through Inelastic Electron Tunnelling. *Phys. Rev. Lett.* **2010**, *105*, 076101.

[13] Y. Kim, K. Motobayashi, T. Frederiksen, H. Ueba, M. Kawai, Action spectroscopy for single-molecule reactions – Experiments and theory. *Prog. Surf. Sci.* **2015**, *90*, 85–143.

[14] B. C. Stipe, M. A. Rezaei, W. Ho, S. Gao, M. Persson, B. I. Lundqvist, Single-Molecule Dissociation by Tunnelling Electrons. *Phys. Rev. Lett.* **1997**, *78*, 4410–4413.

[15] S. G. Tikhodeev, H. Ueba, Relation between inelastic electron tunnelling and vibrational excitation of single adsorbates on metal surfaces. *Phys. Rev.* B **2004**, *70*, 125414.

[16] T. Kumagai, A. Shiotari, H. Okuyama, S. Hatta, T. Aruga, I. Hamada, T. Frederiksen, H. Ueba, Hydrogen relay reactions in real space. *Nat. Mater.* **2012**, *11*, 167–172.

[17] K. Motobayashi, L. Árnadóttir, C. Matsumoto, E. M. Stuve, H. Jónsson, Y. Kim, M.

Kawai, Adsorption of Water Dimer on Platinum(111): Identification of the −OH···Pt Hydrogen Bond. *ACS Nano* **2014**, *8*, 11583–11590.

[18] K. Motobayashi, Y. Kim, R. Arafune, M. Ohara, H. Ueba, and M. Kawai, Dissociation pathways of a single dimethyl disulfide on Cu(111): Reaction induced by simultaneous excitation of two vibrational modes. *J. Chem. Phys.* **2014**, *140*, 194705.

[19] K. Motobayashi, Y. Kim, M. Ohara, H. Ueba, M. Kawai, The role of thermal excitation in the tunnelling-electron-induced reaction: Dissociation of dimethyl disulfide on Cu(111). *Surf. Sci.* **2016**, *643*, 18–22.

[20] J. Oh, H. Lim, R. Arafune, J. Jung, M. Kawai, Y. Kim, Lateral Hopping of CO on Ag(110) by Multiple Overtone Excitation. *Phys. Rev. Lett.* **2016**, *116*, 056101.

[21] T. Huang, J. Zhao, M. Feng, A. A. Popov, S. Yang, L. Dunsch, H. Petek, A Molecular Switch Based on Current-Driven Rotation of an Encapsulated Cluster within a Fullerene Cage. *Nano Lett.* **2011**, *11*, 5327–5332.

[22] J. N. Ladenthin, L. Grill, S. Gawinkowski, Sh. Liu, J. Waluk, & T. Kumagai, Hot Carrier-Induced Tautomerization within a Single Porphycene Molecule on Cu(111). *ACS Nano* **2015**, *9*, 7287–7295.

[23] H. Böckmann, S. Liu, J. Mielke, S. Gawinkowski, J. Waluk, L. Grill, M. Wolf, & T. Kumagai, Direct Observation of Photoinduced Tautomerization in Single Molecules at a Metal Surface. *Nano Lett.* **2016**, *16*, 1034–1041.

[24] D. Novko, M. Blanco-Rey, and J. C. Tremblay, Intermode Coupling Drives the Irreversible Tautomerization in Porphycene on Copper(111) Induced by Scanning Tunnelling Microscopy. *J. Phys. Chem. Lett.* **2017**, *8*, 1053–1059.

[25] T. Kumagai, J.N. Ladenthin, Y. Litman, M. Rossi, L. Grill, S. Gawinkowski, J, Waluk, and M. Persson, Quantum tunneling in real space: Tautomerization of single porphycene molecules on the (111) surface of Cu, Ag, and Au. *J. Chem. Phys.* 2018, **148**, 102330.

[26] B. C. Stipe, M. A. Rezaei, and W. Ho, Coupling of Vibrational Excitation to the Rotational Motion of a Single Adsorbed Molecule. *Phys. Rev. Lett.* **1998**, *81*, 1263–1266.

[27] T. Komeda, Y. Kim, M. Kawai, B. N. J. Persson, H. Ueba, Lateral hopping of molecules induced by excitation of internal vibration mode. *Science* **2002**, *295*, 2055–2058.

[28] M. Parschau, D. Passerone, K. H. Rieder, H. J. Hug, K. H. Ernst, Switching the chirality of single adsorbate complexes. *Angew. Chem. Int. Ed.* **2009**, *48*, 4065–4068.

[29] H. Ueba, Analysis of lateral hopping of a single CO molecule on Pd(110). *Phys. Rev.* B **2012**, *86*, 035440.

[30] T. Frederiksen, M. Paulsson, H. Ueba, Theory of action spectroscopy for single-molecule reactions induced by vibrational excitations with STM. *Phys. Rev.* B **2014**, *89*, 035427.

[31] The square-root of the reduced mass ratio between N–H and N–D is 1.37.

[32] The value of *N* in **Fig. 3b** is slightly different from our previous results in Ref. 9 because we repeated the measurement with the extended range of the tunnelling current to determine the reaction order.

[33] H. Ueba, T. Mii, N. Lorente, and B. N. J. Persson, Adsorbate motions induced by inelastic-tunnelling current: Theoretical scenarios of two-electron processes. *J. Chem.*

Phys. **2005**, *123*, 084707.
[34] Y. E. Shchadilova, S. G. Tikhodeev, M. Paulsson, H. Ueba, Rotation of a Single Acetylene Molecule on Cu(001) by Tunnelling Electrons in STM. *Phys. Rev. Lett.* **2013**, *111*, 186102.
[35] G. Herzberg, Molecular Spectra and Molecular Structure II, Infrared and Raman Spectra of Polyatomic Molecules. (Van Nostrand, Princeton, 1945).
[36] J. G. Radziszewski, J. Waluk, J. Michl, Site-population conserving and site-population altering photo-orientation of matrix-isolated free-base porphine by double proton transfer: IR dichroism and vibrational symmetry assignments. *Chem. Phys.* **1989**, *136*, 165–180.
[37] J. Kügel, L. Klein, M. Leisegang, M. Bode, Analyzing and Tuning the Energetic Landscape of H_2Pc Tautomerization. *J. Phys. Chem. C.* **2017**, DOI: 10.1021/acs.jpcc.7b10564.
[38] S. Bratož, D. Hadži, Infrared Spectra of Molecules with Hydrogen Bonds. *J. Chem. Phys.* **1957**, *27*, 991–997.
[39] Y. Marechal, A. Witkowski, Infrared Spectra of H‐Bonded Systems. *J. Chem. Phys.* **1968**, *48*, 3697–3705.
[40] S. Bratos and H. Ratajczak, Profiles of hydrogen stretching IR bands of molecules with hydrogen bonds: A stochastic theory. II. Strong hydrogen bonds. *J. Chem. Phys.* **1982**, *76*, 77–85.
[41] D. Madsen, J. Stenger, J. Dreyer, E. T. J. Nibbering, P. Hamm, T. Elsaesser, Coherent vibrational ground-state dynamics of an intramolecular hydrogen bond. *Chem. Phys. Lett.* **2001**, *341*, 56–62.
[42] K. Heyne, N. Huse, J. Dreyer, E. T. J. Nibbering & T. Elsaesser, Coherent low-frequency motions of hydrogen bonded acetic acid dimers in the liquid phase. *J. Chem. Phys.* **2004**, *121*, 902–913.
[43] J. Dreyer, Hydrogen-bonded acetic acid dimers: Anharmonic coupling and linear infrared spectra studied with density-functional theory. *J. Chem. Phys.* **2005**, *122*, 184306.
[44] Y. Marechal, IR spectra of carboxylic acids in the gas phase: A quantitative reinvestigation. *J. Chem. Phys.* **1987**, *87*, 6344–6353.
[45] V. Blum, R. Gehrke, F. Hanke, P. Havu, V. Havu, X. Ren, K. Reuter, M. Scheffler, *Ab initio* molecular simulations with numeric atom-centered orbitals. *Comput. Phys. Commun.* **2009**, *180*, 2175.
[46] J. P. Perdew, K. Burke, M. Ernzerhof, Generalized Gradient Approximation Made Simple. *Phys. Rev. Lett.* **1996**, *77*, 3865–3868.
[47] H. J. Monkhorst, J. D. Pack, Special points for Brillouin-zone integrations. *Phys. Rev.* B **1976**, *13*, 5188–5192.
[48] A. Tkatchenko and M. Scheffler, Accurate Molecular Van Der Waals Interactions from Ground-State Electron Density and Free-Atom Reference Data. *Phys. Rev. Lett.* **2009**, *102*, 073005.

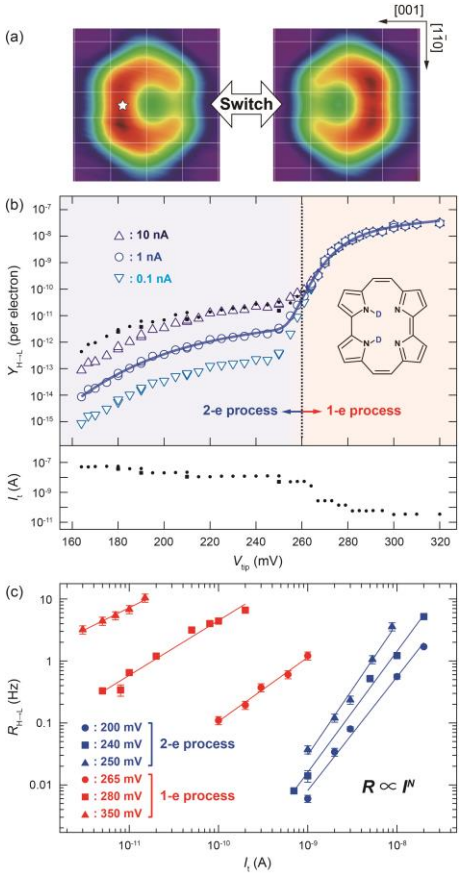

Figure 1. (a) STM images of a single porphycene molecule on Cu(110) at 5 K (V_{tip} = –100 mV, I_t = 10 nA, size: 1.49 × 1.42 nm^2).[10] The white star indicates the tip position during the STM-AS and the conductance measurement. The white grid lines represent the surface lattice of Cu(110). (b) STM-AS for d_2-porphycene on Cu(110) measured at 5 K. The small closed circles and squares in the upper panel indicate the raw data obtained at the tunnelling current shown in the lower panel. The open markers in the upper panel are the calculated $Y(V)$ corresponding to a constant current indicated in the figure. The solid curve represents the best fitting result of $Y(V)$ for I_t = 1 nA to Eq. (5) with the parameters listed in Table 1. (c) Current dependence of the tautomerization rates ($R_{H\to L}$) measured at various bias voltages. The slopes (N) are determined as 1.83(±0.11), 2.12(±0.13), 1.95(±0.08), 2.12(±0.13), 1.03(±0.07), 0.88(±0.06) and 0.71(±0.05) at 200, 240, 250, 265, 280, and 350 mV, respectively.

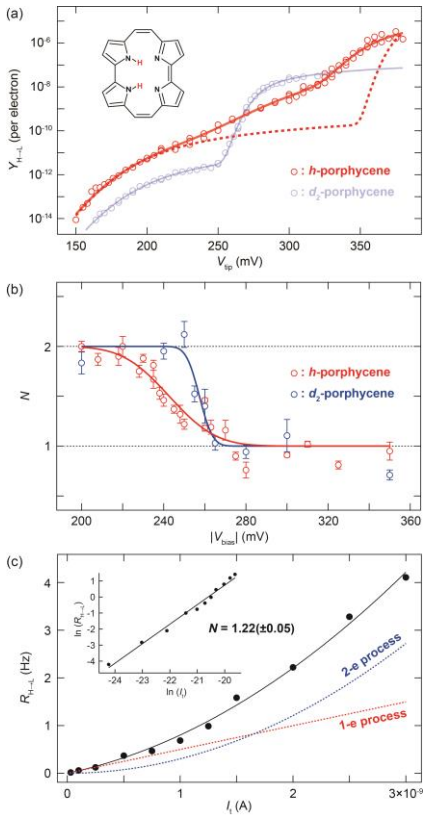

Figure 2. (a) *Y*(*V*) for *h*- and d_2-porphycene on Cu(110) measured at 5 K. The yields in the *N* > 1 regime are normalized to a constant current (1 nA). The dashed red line represents the curve obtained from Eq. (5) using the parameters of ($\hbar\Omega$, σ_{ph}) = (181 meV, 23.2 meV) and (375 meV, 6.8 meV). The solid red line represents the best fitted result with the parameters listed in Table 1. The multiple data points at several bias voltages represent the yields obtained either at different currents or different tip conditions. (b) Voltage dependence of the total reaction order (*N*) for *h*- and d_2-porphycene. The experimental data (symbols) are fitted to a step function convoluted with Gaussian profile. The broadening factors (FWHM) of the Gaussian function are ~42 and ~12 meV for *h*- and d_2-porphycene, respectively. (c) Current dependence of the tautomerization rate measured for *h*-porphycene at V_{sample} = –250 mV. The black solid line is the best fit using Eq. (6), and the dashed lines indicate the contribution from a one- and two-electron process. The inset shows rates on the logarithmic scale.

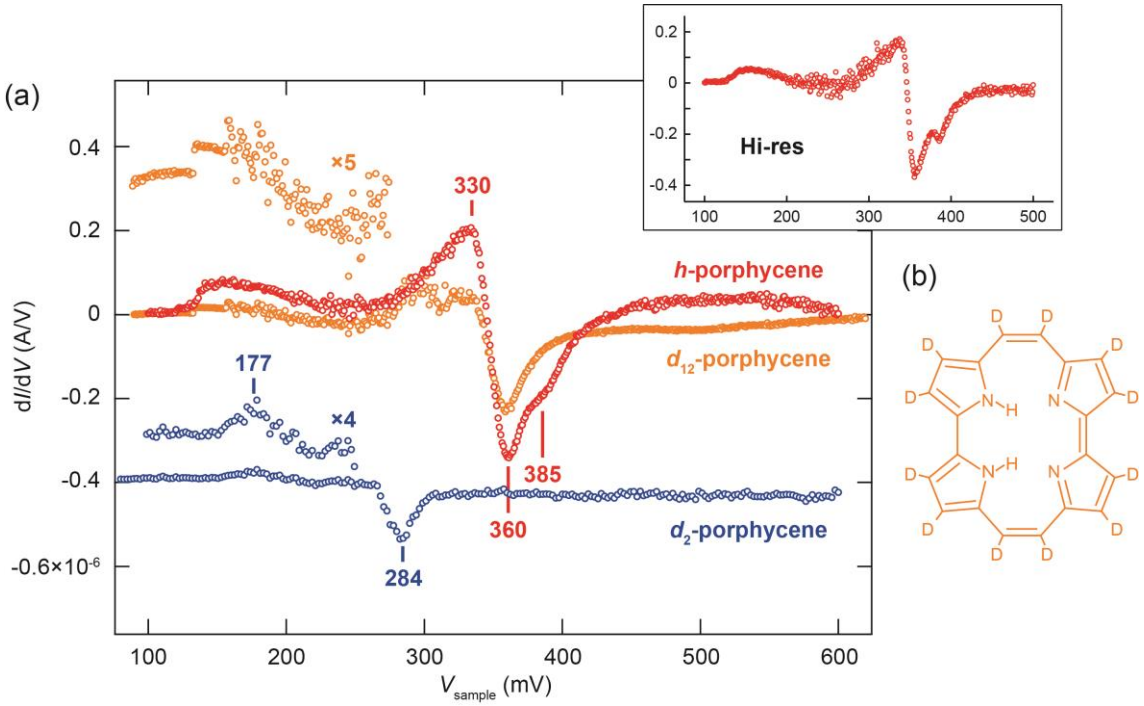

Figure 3. (a) d*I*/d*V* spectra for *h*-, d_2- and d_{12}-porphycene. The spectra over the molecule are subtracted with the background spectra measured over the Cu(110) surface. The tip was fixed at the position indicated in Fig. 1a with a gap condition of V_{sample} = 100 mV and I_t = 20 nA. The spectra were recorded using a lock-in amplifier with a modulation voltage of 12 mV at 710 Hz frequency. The upper inset shows the high-resolution d*I*/d*V* spectrum for *h*-porphycene recorded with a modulation voltage of 3 mV. (b) Chemical structures of d_{12}-porphycene.

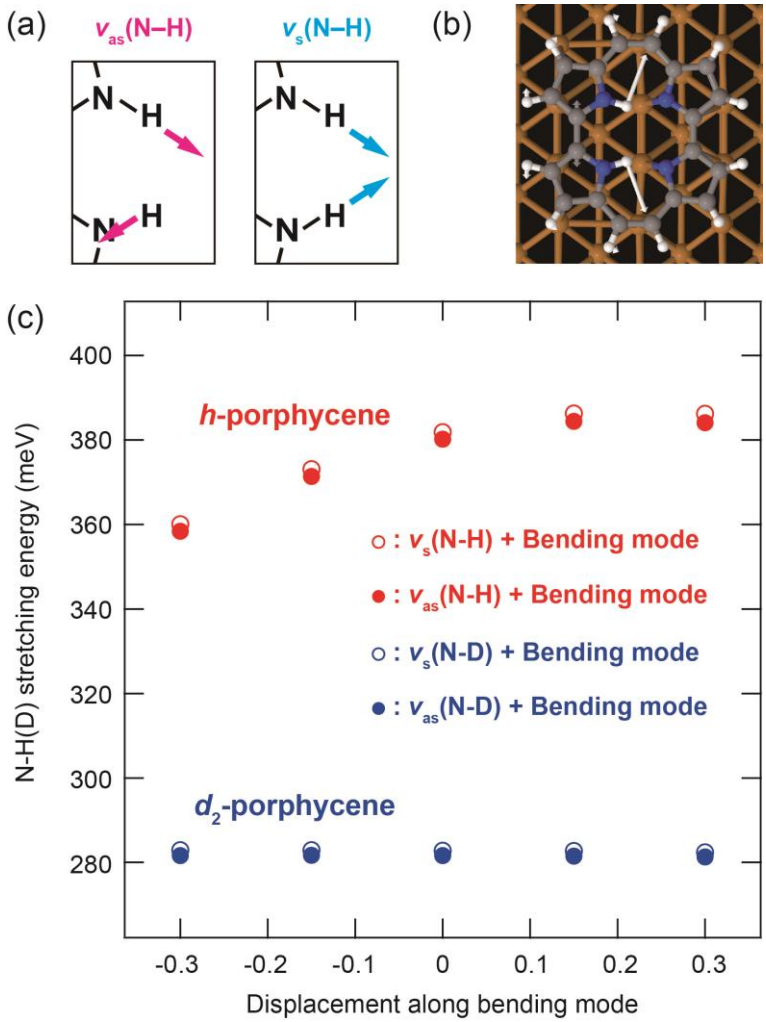

Figure 4. (a) Schematic of anti-symmetric and symmetric *ν*(N–H) (b) Calculated bending mode at 193.5 (186.6) meV for *h*-(*d*2-)porphycene on Cu(110). (c) Variation of the *ν*(N–H) and *ν*(N–D) energies as a function of the displacement along the bending mode. The horizontal axis represents the normal coordinate of the bending mode, which is normalized by its root-mean-square vibrational amplitude of the ground state.